ISSN 0016-7932, Geomagnetism and Aeronomy, 2007, Vol. 47, No. 4, pp. 409–422. © Pleiades Publishing, Ltd., 2007.
Original Russian Text © G.A. Kotova, 2007, published in Geomagnetizm i Aeronomiya, 2007, Vol. 47, No. 4, pp. 435–449.

The Earth's Plasmasphere: State of Studies (a Review)

G. A. Kotova

Space Research Institute, Russian Academy of Sciences, Profsoyuznaya ul. 84/32, Moscow, 117810 Russia

Received November 13, 2006

Abstract—The main results of the experimental and theoretical studies of the Earth's plasmasphere physics obtained until the present are reviewed. The review is aimed at attracting attention of scientists to studying this region of the Earth's magnetosphere since many problems of the plasmasphere physics, first of all, the problems of plasmapause formation and plasmasphere filling and erosion, which are of importance in understanding the relation of the processes proceeding in the Sun and solar wind to the processes observed in the Earth's ionosphere and atmosphere, remain unclear.

PACS numbers: 94.30.cv

DOI: 10.1134/S0016793207040019

1. INTRODUCTION

The plasmasphere is the inner region of the magnetosphere, the form of which resembles torus. Cold plasma with an energy lower than 1–2 eV and a density of 100–1000 cm^{-3}, trapped by the geomagnetic field, plays the dominating role in this region. Hydrogen ions with 10–20% of helium and 5–10% of oxygen ions mainly compose the plasmasphere, which is essentially the extension of the ionosphere to high altitudes [Lemaire and Gringauz, 1998]. It is customary to assume that the plasmasphere begins from an altitude of ~1000 km, where hydrogen ions replace oxygen ions and became the main plasma component. The plasma flowing upward from the ionosphere remains at field lines corotating with the Earth and forms a cloud of cold thermal plasma around the Earth, extending to distances of 4–6 Earth's radii (R_E). Plasma flows are, on average, directed upward (from the ionosphere to the plasmasphere) in daytime and downward (from the plasmasphere to the ionosphere) at night.

The history of the discovery and study of the topside ionosphere and plasmasphere began in the late 1940s–early 1950s. Before that time, nobody suspected that the Earth's ionosphere extends over large distances along the geomagnetic field lines. It was assumed that plasma density rather rapidly decreases above the ionospheric *F* region maximum [Gringauz, 1958]. Based on studying the whistler propagation along the geomagnetic field, Storey [1953] concluded that the electron density at an altitude of ~12000 km in the equatorial region is about 400 cm^{-3} and assumed that he measured the density in the interplanetary space (in that case particle energy was unknown).

In 1958, the experiments performed on the SPUTNIK-3 using charged particle traps [Gringauz et al., 1961] indicated that the ion density above the *F* region (at an altitude of ~1000 km) is ~10^3 cm^{-3}. On the Luna 1 and 2 spacecraft [Gringauz et al., 1960], it was for the first time obtained that plasma with an energy of ~1 eV is registered up to altitudes of ~$4R_E$. A surprisingly sharp outer boundary, where plasma density decreases by an order of magnitude over a distance of several tenths of the Earth's radii, was also discovered.

Based on the whistler studies, Carpenter [1963] detected a sharp decrease in the electron density in the geomagnetic equator plane, initially called "a knee". This knee was identified with the region of a sharp decrease in the ion density discovered on the Soviet satellites [Carpenter, 1965]. Carpenter [1966] subsequently proposed the terms "plasmasphere" and "plasmapause" by analogy with the terms "magnetosphere" and "magnetopause", which were accepted by the scientific community.

An extensive experimental material, obtained on the satellites (Electron-2, -4; z-series; Interball-1, -2; Magion-1; OGO 1–5; ISSE-1, -2; GEOS-1, -2; DE-1; CRRES; IMAGE; et al.,) and using the ground-based methods, has been accumulated since the time of the plasmasphere discovery. The main experimental data on the plasma distribution in the Earth's plasmasphere, plasmapause position, and thermal structure of the plasmasphere will be considered below. The main theoretical concepts of the physics of the plasmasphere and plasmapause will be briefly presented.

2. PLASMA DENSITY IN THE PLASMASPHERE. OBSERVATIONS

A change in the parameters of the plasmasphere is usually considered depending on the McIlwain parameter, *L* (a distance (in the Earth's radii) from the Earth's

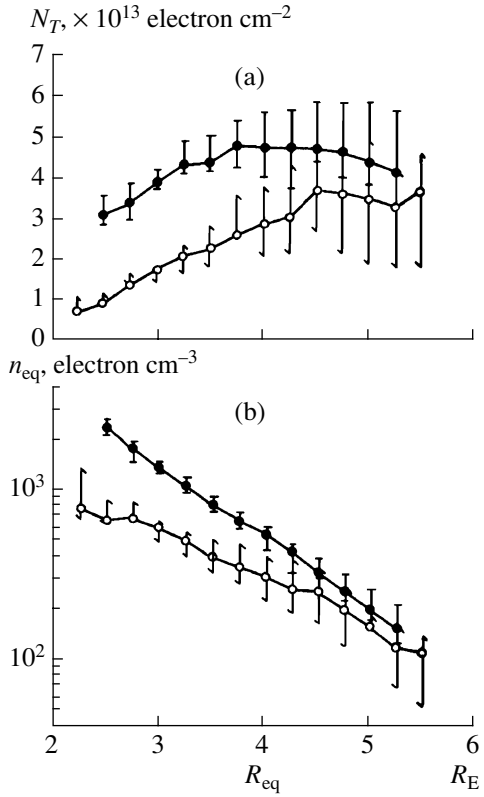

Fig. 1. (a) Average monthly values of total electron content in a flux tube depending on the distance to the tube at the equator according to the whistler measurements near the 75 W meridian in the Antarctic Regions. (b) The corresponding electron density at the equator [Park et al., 1978]. Filled circles were obtained from the measurements performed in November–December 1964; open circles correspond to the June 1965 measurements.

center to a measuring point projected on the geomagnetic equator plane along the magnetic field) and invariant latitude, Λ (a geomagnetic latitude of the field line base on the Earth's surface. In a dipole approximation, $L = 1/\cos^2\Lambda$.

Ion density distribution in the plasmasphere has been studied rather thoroughly since this parameter can be obtained during almost any measurements in the plasmasphere. The first experiments indicated that plasma density distribution strongly depends on geomagnetic activity [Lemaire and Gringauz, 1998]; therefore, we first consider plasma distribution under quiet geomagnetic conditions.

The ion density distribution in the geomagnetic equator plane has been thoroughly studied based on the whistler observation data. The method for determining plasma parameters based on whistler observations was considered by D. Carpenter (see [Carpenter, 2004] and references therein). The ion and electron density was also determined in the wave and plasma experiments on the satellites [Gurnett et al., 1979; Chappel et al., 1981; Gringauz and Bezrukikh, 1977; Gringauz and Bassolo, 1990; Kotova et al., 2002; and others].

Under quiet geophysical conditions near the geomagnetic equator plane, cold plasma density decreases with increasing distance from the Earth, and a sharp outer plasmaspheric boundary is often not observed and density smoothly decreases in the cases when magnetic conditions remain quiet during several days. The density decrease rate ($d\log N_{eq}/dL$) varies from –4 to –3 [Tarcsay et al., 1988; Carpenter and Andersen, 1992; Kotova et al., 2002; and others].

Plasma density in the plasmasphere depends on local time, latitude, and observation season. According to [Park et al., 1978], the density daily variations near the equator are ±10–15% for $L \sim 3$, and the density is minimal after midnight.

According to whistler observations, which make it possible to almost continuously monitor the equatorial plasmasphere, annual density variations were revealed in the inner plasmasphere. The ratio of the maximal December density to the minimal June density can reach 2 near $L = 2.5$ (Fig. 1). Whistler observations also indicate that plasma density (in the inner plasmasphere too, $L < 2.5$–3.0) substantially depends on the phase of solar activity. At $L \sim 2$, the ratio of the electron density near the equator at a solar cycle maximum to the density at a solar minimum is ~1.5.

A change in plasma density in the plasmasphere along the magnetic field lines has been rather poorly studied experimentally. Based on a statistical analysis of the DE-1 satellite data, Gallagher et al. [2000] assumed that plasma density insignificantly changes along magnetic shells at $L > 3$, beginning from an altitude of 1 R_E; however, a performed analysis did not share data on geomagnetic activity and local time. The first experimental plasma distributions along the magnetic field lines were factually obtained based on data of IMAGE/RPI (radio plasma imager) radio sounding [Tu et al., 2003]. The density distributions along L = 2.2–3.2 field lines indicate that density insignificantly changes at geomagnetic latitudes of ±20–25° at least in the morning plasmasphere and subsequently increases by a factor of 1.5–2 toward latitudes of ~±40°, which corresponds to altitudes of ~4000–5000 km.

3. PLASMA DENSITY IN THE PLASMASPHERE. THEORETICAL CONCEPTS

Several empirical models of density distribution depending on L, local time, observation season, and geomagnetic activity level were constructed based on a large volume of accumulated experimental data on plasma density in the Earth's plasmasphere [Carpenter and Anderson, 1992; Gallagher et al., 2000]. The analytical expression, obtained based on an analysis of

ISEE-1 data and whistler observations [Carpenter and Anderson, 1992], can be used in estimations:

$$\begin{aligned}\log N_{eq}(L, d, \tilde{R}) &= -0.3145L + 3.9043 \\ &+ 0.15\cos[2\pi(d+9)/365]\exp[-(L-2)/1.5] \\ &- 0.5\cos[4\pi(d+9)/365]\exp[-(L-2)/1.5] \\ &+ (0.00127\tilde{R} - 0.0635)\exp[-(L-2)/1.5],\end{aligned} \quad (1)$$

where d is the serial number of a day in year, and $\tilde{R}$ is the average sunspot number for 13 months. This formula describes plasma density near the geomagnetic equator during a prolonged geomagnetically quiet period for 0000–1500 MLT.

Several theoretical models of filling and maintenance of the Earth's plasmasphere have been proposed and developed. Ionospheric plasma is mainly caused by hydrogen ions produced during the recharge of hydrogen atoms with oxygen ions in the resonance reaction: $H + O^+ \longleftrightarrow H^+ + O$. This reaction proceeds identically rapidly in both directions. A chemical equilibrium is formed at low altitudes (the F region and slightly higher) where oxygen density is rather high. However, in the electric field of ambipolar diffusion, which is generated in the gravitational field by dominating oxygen ions and electrons, produced hydrogen ions move upward along magnetic field lines [Bauer, 1973; Lemaire and Gringauz, 1998]. Thus, the polar wind originates at high latitudes, where field lines extend far into the tail, and the Earth's plasmasphere is formed at closed field lines. The processes of ionospheric–plasmaspheric exchange with charged particles are decisive in the dynamics of the plasmasphere.

Ionospheric models are rather adequately developed and take into account photochemical processes, processes of recombination and ion interaction with neutrals, thermospheric winds, etc. [Schunk and Sojka, 1996]. When a model of plasma distribution in the plasmasphere is constructed, either parameters of the neutral atmosphere and ionosphere are used as input parameters or a general ionospheric–plasmaspheric model is constructed. Both hydrodynamic [Krinberg and Tashchilin, 1984; Richards and Torr, 1988; Bailey et al., 1997; Tu et al., 2003; Webb and Essex, 2004] and kinetic (or quasikinetic) [Pierrard and Lemaire, 1996; Khazanov et al., 1998; Reynolds et al., 2001] approaches are used.

Lemaire with coauthors [Lemaire and Gringauz, 1998; Lemaire, 1999; Pierrard and Lemaire, 2001] considered limiting cases of plasma density distribution in a stationary plasmasphere: a model of diffusion equilibrium and an exospheric model. An analysis indicated that the hydrostatic diffusion equilibrium, where the total plasma flow along the magnetic field is zero, cannot reproduce observed density distributions in the plasmasphere even when a geomagnetically quiet period is prolonged. The experimental density profiles, obtained from the ISSE-1 spacecraft data near the geomagnetic equator under the conditions of a prolonged quiet period, are characterized by a constant exponential density decrease rate [Lemaire, 1999; Carpenter and Anderson, 1992], whereas the density calculated for the conditions of diffusion equilibrium decreases much slower and even starts increasing at $L > L_0 = 6.6(\Omega_E/\Omega)^{2/3}$, where Ω_E and Ω are the angular velocities of rotation of the Earth and plasmasphere, respectively. A plasma density minimum was not observed experimentally up to $L = 8$. It was also indicated that density distributions become unstable relative to the interchange and quasi-interchange instabilities at $L > L_0$. Nevertheless, a diffusion equilibrium model is applicable in the inner plasmasphere ($L < 3$) [Lemaire and Gringauz, 1998].

Using a diffusion equilibrium model, Angerami and Thomas [1964] indicated that density distribution in the plasmasphere strongly depends on the ion composition of the ionosphere at the flux tube base at an altitude of ~500 km. Analyzing the annual variations in the plasmaspheric density (Fig. 1), Guitter et al. [1995] arrived at the conclusion that these variations are most probably related to O^+ ion density variations in the ionosphere, in turn, caused by seasonal changes in the composition of the neutral atmosphere. Although, the other explanation, related to a plasmaspheric electron temperature rise in December, is also possible [Richards et al., 2000].

A model of expansion into free space, or an exospheric model, represents the other limiting case. In such a model, it is assumed that particles move without collisions above a certain critical level. Depending on the initial kinetic energy and pitch angle, particles can move along ballistic, escaping (or precipitation), and closed trajectories. In diffused equilibrium models, particles moving along different trajectories are in a thermal equilibrium; i.e., the distribution function is everywhere isotropic. Due to a lower probability of Coulomb collisions at high altitudes (the time between Coulomb collisions is larger than the time of particle motion between hemispheres) in exospheric models, trapped particles can be partially or absolutely absent, but the distribution function remains symmetrical about the velocity component, and the total particle flux is zero. Pierrard and Lemaire [2001] indicated that an exospheric model, considering particle distribution functions in which the contribution of trapped particles depends on L, can explain observed steady-state profiles of ions in the equatorial plasmasphere. If trapped particles are absolutely absent, an exospheric model describes the minimal density profile of particles filling the plasmasphere in the time during which a thermal ion passes between hemispheres.

The FLIP (field line interhemispheric plasma) model [Tu et al., 2003] was used to analyze the electron density distributions along field lines, obtained during IMAGE radio sounding. This model solves the equations of continuity and momentum and energy conser-

vation for O^+, H^+, He^+, and N^+ ions along field lines of an inclined dipole from an altitude of 120 km in both hemispheres. A comparison was performed for the measurements carried out on June 8 along field lines of L = 2.51, 3.0, and 3.23 after the magnetic disturbance with Kp = 5.3. The calculated density values in the regions distant from the equator proved to be much lower than the observed values, although good agreement was reached near the equator. To obtain agreement in the regions outside the equator, the authors assumed that an additional source of ion heating exists in the equatorial region of the plasmasphere [Tu et al., 2003]. Thus, it was anyhow indicated that theoretical models can be verified if they are compared with observations not only in the equatorial region but also along the entire flux tube.

4. STRUCTURAL FEATURES OF DENSITY DISTRIBUTION IN THE PLASMASPHERE

Based on the Prognoz satellite data, Gringauz and Bezrukikh [1976] detected the noon–midnight asymmetry of the plasmasphere. The daytime $N(L)$ profile is often gentler than the nighttime profile. The noon–midnight asymmetry is usually observed at low and moderate magnetic activity. A difference in the properties of the noon and midnight regions was confirmed by the data of other satellites [Decreau et al., 1982]. According to the ISEE-1 satellite data [Carpenter and Anderson, 1992], a difference between the distance to the dayside and nightside plasmasphere is not more than 0.5 R_E, which does not contradict the Prognoz data [Gringauz and Bezrukikh, 1977] since only sharp boundaries in the plasmasphere were considered. Moreover, the data of the ISEE-1 and other satellites indicate that the plasmapause is most sharp and smooth on the nightside and dayside, respectively.

The first experimental data indicated that a bulge is observed in the plasmapause shape on the dusk side, and this bulge is maximal during magnetically disturbed periods and shifts to earlier hours with increasing magnetic activity [Carpenter, 1966]. A detailed consideration of the plasma density profiles on the dusk side of the plasmasphere according to the DE-1, ISEE-1, and GEOS-2 satellite data led to the conclusion [Carpenter et al., 1993] that, during disturbed periods, the dusk side of the plasmasphere is topologically composed of the "main" plasmasphere and the bulge region. During a prolonged quiet period, a dusk bulge is almost absent, the plasmapause shape in the equatorial plane is close to a circle, and the dusk radius of this circle is larger than the dawn radius by only ~0.5 R_E. A similar result was obtained when plasmapause crossings by ISEE-1 were considered [Carpenter and Anderson, 1992]. The region of a dusk bulge is very irregular, and isolated plasma patches are usually observed here. Along the satellite orbit, these patches of a dense cold plasma are separated from the main plasmasphere by the regions with a very low-density cold plasma. Such "peaces" of the plasmaspheric plasma are also often observed on geostationary satellites near the magnetopause, usually in the postnoon sector, during several days after a magnetic storm (e.g., on GEOS-2 [Higel and Wu, 1984]). Direct measurement on satellites as well as wave observations of whistlers do not make it possible to distinguish isolated plasma regions from more complicated formations, which can actually be a continuation of the plasmasphere and somewhere join the plasmasphere.

This problem was elucidated using the data of the IMAGE spacecraft, which was launched in 2000. The EUV (extreme ultraviolet imager) device made it possible to photograph the plasmasphere in a resonantly scattered helium emission (30.4 nm) [Sandel et al., 2003]. Four main types of structures in the density distribution in the plasmasphere were revealed: density notches and channels, a shoulder on the plasmapause equatorial projection, and plasmaspheric tails or plumes.

A comparison of the plasmaspheric images in the 304 nm line with the data of the RPI radio sounding of the plasmasphere on the same satellite indicated that "separated pieces of the plasmasphere" and plumes were identically registered by both RPI and EUV devices (Fig. 2). From this comparison the conclusion was also made that the region of increased plume density is not only bounded by the equatorial plane but also extends to, at least, 38° latitude [Sandel et al., 2003]. The conclusion that "separated pieces of the plasmasphere" extend along flux tubes was previously drawn in [Kotova et al., 2002a].

Channels are narrow regions of decreased plasma content extended along latitude (Fig. 2). First, channels appear in the premidnight sector but sometimes extend through the midnight meridian into the early dawn sector. Channels are possibly generated after plumes, when the latter begin to twist around the plasmasphere [Sandel et al., 2003].

A "shoulder"—an asymmetric bulge at the plasmapause with a sharp boundary on the eastern side (a change in the plasmapause radius $\Delta R \sim 0.5 R_E$)—was an unusual plasmaspheric structure observed from the IMAGE satellite.

Density notches (bite-out, voids) are narrow, restricted in latitude, devastated regions (flux tubes) of the plasmasphere (Fig. 3). Caverns occupy less than ~10°–30° in longitude and extend from $L \sim 2$–3 to the plasmaspheric boundary in the adjacent denser regions [Sandel et al., 2003]. Density caverns were registered from the data of an analyzer with a decelerating potential on the Magion-5 satellite using the direct methods [Kotova et al., 2004]. The Magion-5 data also indicate that the temperature in the regions of decreased density is higher than in the adjacent denser regions of the plasmasphere. A density notch shape remains usually unchanged during their lifetime. The observations of notches were used [Sandel et al., 2003] to determine the

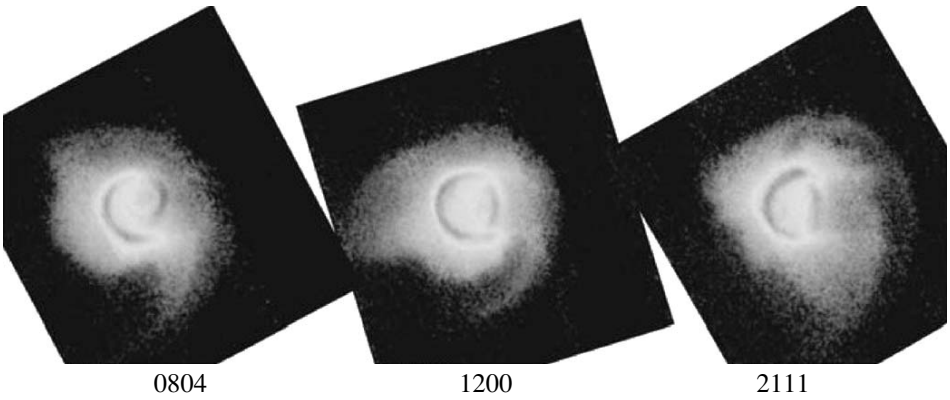

Fig. 2. The EUV/IMAGE photographs of the plasmasphere in the 30.4 nm line obtained on June 10, 2001; the universal time of photographing is indicated below. The Sun is located on the left. Plume rotates around the plasmasphere and a channel is formed as a result of the plasmasphere corotation with the Earth [Sandel et al., 2003].

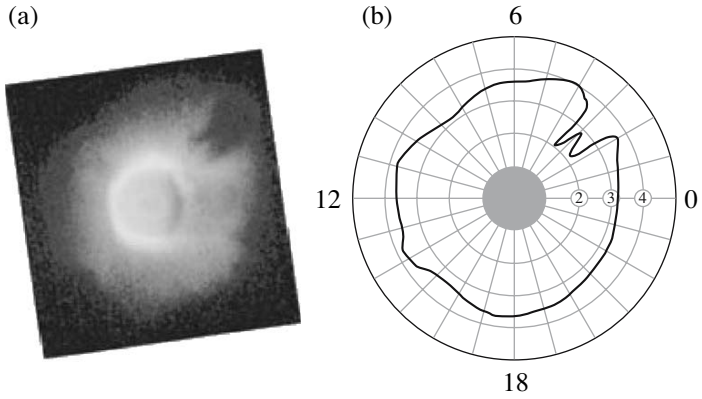

Fig. 3. (a) The EUV/IMAGE photograph of the plasmasphere with a density notch in the 30.4 nm line, obtained at 1710 UT on June 24, 2000. The Sun is on the left. (b) Brightness (approximately plasmapause) boundary projection onto the geomagnetic equator plane in the *L*–MLT coordinates [Sandel et al., 2003].

plasmasphere corotation velocity. It was discovered that, at $1 < L < 4$, the plasmasphere rotation velocity accounts for 85–90% of the velocity of corotation with the Earth and is not always constant. Rotation velocities of long-lived caverns are comparable with drift velocities in the topside ionosphere measured on DMSP satellites; i.e., caverns lag behind the corotation with the Earth apparently due to ionospheric processes [Burch et al., 2004]. A comparison of the RPI and EUV data from the IMAGE spacecraft indicated that the kilometric emission is generated within density caverns in the geomagnetic equator region near the plasmapause.

5. PLASMAPAUSE POSITION, PLASMASPHERE DEPLETION AND REFILLING

Figure 4 schematically presents a change in the electron density equatorial profile and a plasmapause motion during geomagnetic disturbances [Carpenter and Park, 1973]. Profiles *1* and *2* can be considered as limiting density changes under quiet conditions before and immediately after a magnetic storm. A change in the plasmapause position (a sudden, by more than an order of magnitude, change in the density at distances of several fractions of *L*) occurs during several hours. Profile reconstruction, i.e., filling of the plasmasphere, is a much slower process proceeding during several days. The second, weaker, geomagnetic storm occurs when the plasmasphere is still incompletely filled, and a step is formed on profile *5*. During strong storms, the plasmapause can approach the Earth up to $L = 2.0$ [Lemaire and Gringauz, 1998]. During quiet periods, the profile can extend ($N > 10$ cm^{-3}) to $L > 8$, and a sharp decrease in the density–plasmapause can be invisible [Gringauz and Bezrukikh, 1976]. Usually, plasma density in the plasmasphere also decreases as a result of a storm [Carpenter and Lemaire, 1997; Bezrukikh et al., 2001]. According to the ISEE-1 data, the plasmapause thickness is 250–1250 km and is almost independent of the plasmapause position (L_{pp})

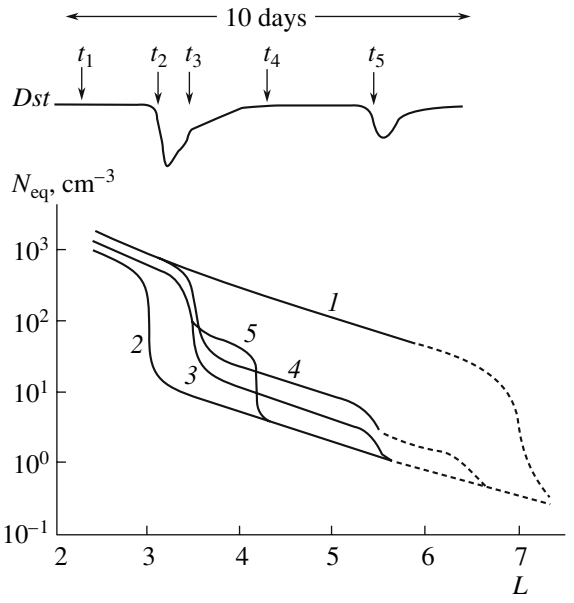

Fig. 4. Schematic change in the electron density equatorial profile during the 10-day period including two magnetic storms. The series of profiles is marked by numerals corresponding to the instants shown on the *Dst* variation profile. The profiles correspond to the conditions at about 0400 MLT [Carpenter and Park, 1973].

when the boundary is identified distinctly. The sharpest and largest density jumps at the plasmapause are observed on the nightside [Gringauz and Bezrukikh, 1976; Carpenter and Anderson, 1992].

Plasmapause position is most often determined from the expression [Carpenter and Anderson, 1992]:

$$L_{pp} = 5.6 - 0.46Kp_{\max}, \quad (2)$$

where L_{pp} is the L value of the last point measured on the density profile before a sharp density drop at the plasmapause, and $Kp_{\max}$ is the maximal Kp value during 24 h before measurements. However, if measurements were related to sectors in the vicinity of 09, 12, or 15 MLT; the corresponding Kp values for one, two, or three preceding 3-h intervals were ignored in order to take into account the observed delay of the response of the dayside plasmapause position to geomagnetic activity (see, e.g., [Décréau et al., 1982]). Formula (2) is applicable to $0 < \text{MLT} < 15$. The observations of whistlers and satellite measurements indicate that short-term substorms cause plasmapause to shift toward the Earth in a small region in the nightside and early dawn sector. Correspondingly, changes in the plasmapause position in other MLT sectors are observed with a delay equal to a corotation time [Carpenter and Park, 1973, Carpenter and Lemaire, 1997]. If substorm activity is prolonged, the entire plasmasphere decreases, and the plasmapause starts moving toward the Earth, apparently, simultaneously on the night and day sides but maximally approaches the Earth, first, on the nightside and, ~12 h later, on the dayside [Bezrukikh et al., 2001].

From the IMAGE data during the storm of July 10, 2000, Goldstein et al. [2003] managed to determine the radial velocity of erosion (the maximal velocity was observed at 2.4 MLT) of the nightside plasmasphere (~0.6 R_E h^{-1}); the periods of plasmapause shift toward the Earth (erosion) corresponded to the registration of the IMF southward component (the remaining components were approximately constant at that time) with regard to delays of 3.7 min for the solar wind propagation to the magnetopause and 30 min for the plasmapause response.

According to the Park [1974] estimates, the number of electrons lost by the plasmasphere during a magnetic storm is about 10^{31}, if shells were depleted from $L = 3.5$ to $L = 5.0$ and the total electron content in a tube with a section of 1 L at an altitude of 1000 km was 5×10^{13} within $L = 5$ before a disturbance. Apparently, the loss is mostly caused by cross-field plasma convection at an increased electric field. Plumes are observed evidences of such a process. It is still unclear whether plasma carried out of the plasmasphere is lost in the boundary layers of the magnetopause or remains trapped in the plasma sheath. Part (what?) of plasma lost by the plasmasphere during erosion is probably discharged into the ionosphere, and this process should also proceed both outside and within a newly generated plasmapause [Carpenter and Lemaire, 1997].

The plasmasphere is filled due to fluxes from the ionosphere, and (see above) this process is much slower than the process of erosion (Fig. 4). The whistler observations indicate that, under quiet conditions, the process of filling is rather homogeneous: the total electron content in plasmaspheric tubes with a section of 1 cm^2 from an altitude of 1000 km increases by ~5×10^{12} particles per day. The time of plasmasphere filling changes from ~1 day for $L = 2.5$ to ~ 8 days for $L = 4$. According to Carpenter et al. [1993], the rate of plasmasphere filling at $L = 4.5$ near the equator remains about 80 cm^{-3} per day for several days after a small magnetic storm. From the GOES-2 data [Song et al., 1988] it was found that the rate of plasmasphere filling in geostationary orbit is inversely proportional to the absolute value of the *Dst* index and is about 10–25 cm^{-3} per day; i.e., filling (to 70.5 cm^{-3}) occurs within 3–7 days. The latter data of the IMAGE spacecraft confirmed Park's estimates. According to the RPI data, the plasmasphere is filled during ~28 h at $L = 2.8$ [Green and Reinisch, 2003]. All these experimental estimates do not correspond to the calculated times of plasmasphere filling, which are much longer. For example, according to [Rasmussen, 1993], the time of atmosphere filling is ~3 and 100 days at $L = 3$ and 5, respectively. Such discrepancies confirm that the plasmaspheric density is far from the saturation level and indicate that it is necessary to create models corresponding better to experimental data.

6. PLASMAPAUSE MODELS

Theoretical models of plasmapause formation are usually based on magnetic hydrodynamic assumptions. Magnetic field lines are considered equipotential (**EB**) = 0. Gradient and centrifugal particle drifts can be neglected and only drift in cross fields ($v_E = \mathbf{E} \times \mathbf{B}/\mathbf{B}^2$) can be considered for cold plasma ($T \sim 0$, $\beta \sim 0$). An insignificant gravitational drift is also ignored. The field generated by plasma rotation in the geomagnetic field in a stationary coordinate system and the sunward plasma convection field, existing due to the interaction between the solar wind and the magnetosphere, are the main electric field components in the magnetosphere.

In the first theoretical models, the cold plasma boundary—plasmapause—was identified with the last closed equipotential surface of superposition of the corotation electric field and a homogeneous field of dawn–dusk magnetospheric convection [Nishida, 1966; Brice, 1967]. In the inner magnetosphere, the geomagnetic field can be considered dipole and (neglecting a dipole inclination with respect to the Earth's rotation axis) the magnetic dipole value in the equatorial plane is $B = B_0 R_E^3/r^3$ (where $B_0 = 0.312$ G is the magnetic field on the Earth's surface at the equator, and r is the distance to a measuring point. After corotation, $E_{cor} = -(\mathbf{\Omega}_E \times \mathbf{r}) \times \mathbf{B}$ at the equator is directed radially toward the Earth's center (Ω_E is the Earth's rotation angular velocity). Electric fields are summed up on the dawn side and are subtracted on the dusk side, as a result of which a dusk bulge is formed. The radial distance from the flux stagnation point can be estimated as $r_0^2 = \Omega_E B_0 R_E^3/E$.

The later calculations of the plasmapause position are based on more complicated electric field models in the magnetosphere: both theoretical models, based on the solution of the Poisson equation with boundary conditions in the ionosphere and magnetosphere, and empirical models, based on electric field measurements on geostationary and low-orbiting satellites and during ground-based radar experiments (see [Liemohn et al., 2004] and references therein). The external convection electric field shielding near the plasmapause due to the gradient and centrifugal drift of ring current ions and electrons with a nonzero temperature in the geomagnetic field and the existence of field-aligned currents from the ionosphere in the dawn sector and into the ionosphere in the dusk sector are also taken into account [Kivelson and Russel, 1995; Block, 1966; Karlson, 1971; Spiro et al., 1981].

MHD models of plasmapause formation [Grebowsky, 1970; Chen and Wolf, 1972] indicated that extended plasmaspheric tails, which should constantly be generated on the dusk side during magnetic disturbances, can exist (Fig. 5). However, nobody could satisfactorily explain experimentally observed dimensions and position of isolated plasma clouds, possibly, somewhere combined with the plasmasphere [Chen and Grebowsky, 1978].

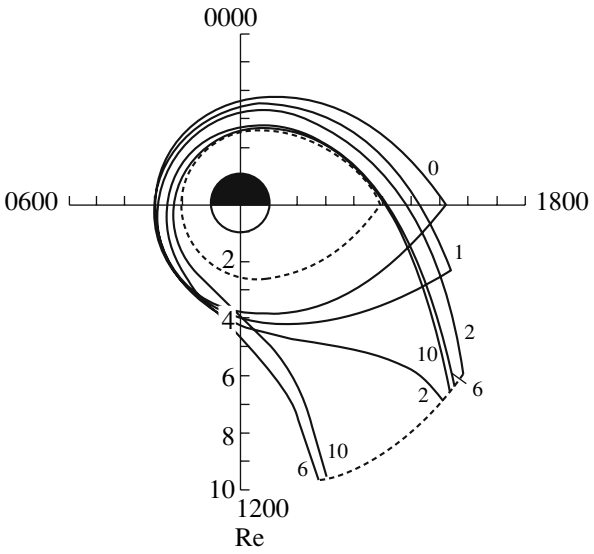

Fig. 5. The plasmapause position at the selected instants (0, 1, 2, 6, 10 h) in the equatorial plane *R*–LT after a sudden increase in the dawn–dusk electric field from 0.28 to 0.58 mV m^{-1} [Grebowsky, 1970]. Dots indicate the final plasmapause position.

These models are simple and attractive; nevertheless, several difficulties arise when these models are used. A considerable dawn–dusk asymmetry of the plasmapause, which is almost absent in the experimental data under prolonged undisturbed conditions (see above), exists in such a model under quiet conditions. A model identifying the plasmapause with the last closed equipotential surface does not explain the existence of a noon–midnight asymmetry during undisturbed periods. According to such a model, at a sudden increase in the dawn–dusk electric field (Fig. 5), the plasmapause almost immediately shifts toward the Earth in the dusk sector and approaches the Earth in the midnight and postmidnight time sectors only 6–10 h after an increase in the field [Grebowsky, 1970]. At the same time, the experimental data (e.g., [Carpenter and Park, 1973] indicate that the midnight and early dawn regions of the plasmasphere respond to disturbances most quickly. An Earthward shift of magnetic flux tubes on the nightside during a magnetic storm should lead to an increase in plasma density in tubes, whereas plasma density in the plasmasphere decreases at least during strong storms. Almost arbitrary initial conditions, specifically, convection electric field values, are selected when MHD models are used to calculate the current plasmapause position. Finally, J. Lemaire [Lemaire and Gringauz, 1998, p. 196] indicates that, following a simple hydrodynamic model of formation, the plasmapause should be the sharpest when the electric field distribution is stationary, i.e., under prolonged quiet conditions. However, observations indicate that the

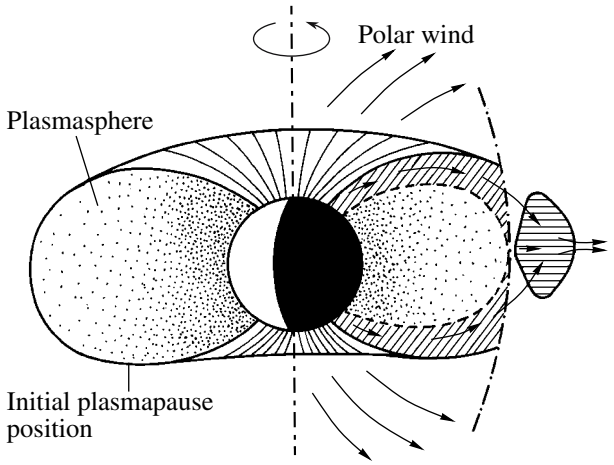

Fig. 6. The upward ionization flux and the separation of the plasma fragment from the plasmasphere as a result of increased magnetospheric convection. Separation is caused by an increase in centrifugal effect in the outer plasmasphere outside the ZPF surface (dot-and-dash) in the postmidnight magnetospheric sector [Lemaire, 2001].

plasmapause can altogether be not observed under such conditions, and a sharp plasmapause is formed during nonstationary processes in the course of magnetic storms.

An alternative hydrodynamic model of plasmapause formation was proposed in [Lemaire and Gringauz, 1998, Section V; ht-tp://plasma.oma.be/plasmapause_deformations/]. This model is also based on the electric field model in the magnetosphere, i.e., on the plasma convection model, but takes into account gravitational force. In this model plasma is identified with and L shell tangent to the "surface of a zero parallel force" (ZPF) (Fig. 6). On the ZPF surface, the components of the gravitational and general centrifugal forces are equalized along the magnetic field. The distance to the ZPF surface in the equatorial plane is $L_c = (2GM_E/3\Omega^2 R_E^3)^{1/3} = 5.78(\Omega_E/\Omega)^{2/3}$, where M_E is the Earth's mass, G is the gravitation constant, and Ω is the real velocity of plasmasphere rotation. The potential energy of charged particles moving along such L shells that $L < L_c$ has one maximum in the geomagnetic equator plane. The potential energy of particles at $L > L_c$ has a local minimum at $\lambda = 0$ (λ is the geomagnetic latitude) and two local maximums at $\lambda = \pm \arccos(L_c/L)^{3/8}$ at crossings of their L shell with the ZPF surface. It was indicated that, outside the plasmapause defined in such a way, plasma escapes into the topside magnetosphere due to the interchange instability; within the ZPF surface, plasma remains trapped and corotates with the Earth.

During magnetospheric substorms or storms, the electric field of magnetospheric convection increases and penetrates into the outer plasmaspheric regions; eastward and sunward plasma convection in the postmidnight magnetospheric sector correspondingly increases. As a result of an increase in the effective rotation velocity of the outer plasmaspheric regions, the ZPF surface approaches the Earth, and plasma from the outer L shells accelerates toward the equatorial plane owing to an increased centrifugal force. As a consequence, thermal plasma, for which $L > L_c$ in this case, flows upward from the topside ionosphere along the entire flux tube. Mainly light H^+ and He^+ ions leave the ionosphere, thereby, forming a trough of light ions in the midlatitude ionosphere [Lemaire, 2001]. Plasma that accumulates at a potential energy minimum near the equatorial plane outside the ZPF surface escapes into the topside ionosphere due to the quasi-interchange instability. The calculations use a model of the electric field dependent on the *Kp* index [McIlwain, 1986].

The plasmapause formation mechanism [Lemaire and Gringauz, 1998] makes it possible to explain a number of observational facts. According to the experimental data, the plasmapause is located at $L \sim 5.6$–5.7 in the absence of geomagnetic disturbances [Carpenter and Anderson, 1992; Carpenter and Park, 1973; Moldwin et al., 2002], which is in good agreement with the model value $L_c = 5.78$. According to this model, changes in the plasmapause position are most sharp on the nightside since up-to-date models of electric field in the magnetosphere indicate that the convection rate during magnetic disturbances is maximal after midnight and the interchange instability increment is inversely proportional to the integral Pedersen conductivity, which is minimal on the nightside. The sharpest magnetospheric boundary is actually observed at and after midnight [Gringauz and Bezrukikh, 1976; Carpenter and Anderson, 1992]; the plasmapause shifts toward the Earth in the postmidnight sector during bursts of the *AE* index (substorm activity) and lags behind *AE* in other time sectors [Carpenter and Park, 1973; Kotova et al., 2004]. The model correctly reflects the relation between the plasmapause position and the *Kp* index since Lemaire used in his calculations the McIlwain empirical model of the convection electric field depending on the *Kp* index [McIlwain, 1986].

The Lemaire model predicts the existence of separated cold plasma patches going out of the plasmaspheric nightside. The channels observed on IMAGE in the nightside sector of the plasmasphere are possibly related to the formation of such bulges. Moreover, density profile irregularities, often observed during direct satellite experiments and whistler observations, not always can be explained by the formation of plasmaspheric tails or plumes.

As was mentioned above, the existence of plumes was reliably confirmed by the IMAGE data. However, the observations indicate that plumes are formed during the westward rotation of a plasmaspheric bulge gener-

ated on the dayside [Goldstein, 2004] rather than due to plasma convection toward the Sun in the dusk sector as MHD models of plasmapause formation predicted (Fig. 5) [Grebowsky, 1970; Chen and Wolf, 1972]. An increase in sunward convection due to an increase in the dawn–dusk electric field results in the formation of a plasmaspheric bulge in prenoon hours, subsequent rotation of this bulge (but with a delay of the outer regions relative to the inner ones), and formation of a plume. Deceleration in the outer regions of the plasmasphere in the afternoon is related to the penetration of the dawn–dusk field into these regions.

The formation of density caverns in the plasmasphere should be related to the effect of a nonstationary local electric field. Nonstationary local electric fields can be generated during substorms mostly in the midnight sector of the plasmasphere [Wygant et al., 1998]. [Pierrard and Lemaire, 2004] explain the formation of density caverns in the plasmasphere by a rapid successive increase and subsequent decrease in the *Kp* value and related variations in the McIlwain electric field [McIlwain, 1986]. Apparently, the formation of density caverns is actually related to an increase in magnetic activity (Fig. 7, [Kotova et al., 2004]); however, the generation of so narrow inhomogeneities in the plasmasphere (<3 MLT) should hardly be described by the 3-h *Kp* index. Gallagher et al. [2005] relate the formation of density caverns to the generation of plasmaspheric tails during the magnetic storm recovery phase. However, density caverns are not always observed at the end of a magnetic storm.

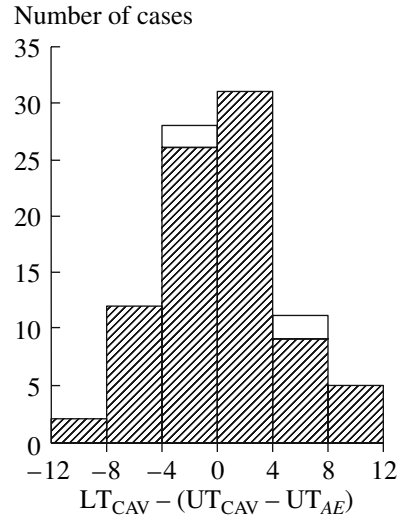

Fig. 7. Distribution of the density notch registration in the plasmasphere on the IMAGE spacecraft (dashed) in May 2000–June 2001 and on Magion-5 depending on a difference between the local time of notch registration (LT_{CAV}) and the time delay of the notch registration (UT_{CAV}) relative to the *AE* burst origination (UT_{AE}).

7. THERMAL STRUCTURE OF THE PLASMASPHERE

The set of data on the ion and electron temperature in the plasmasphere is much smaller than the set of density data since whistler measurements do not make it possible to estimate this parameter, and data on temperature were obtained only during direct satellite experiments. The ion temperature (T_i) in the plasmasphere was first estimated by Gringauz et al. [1960]. Based on the Luna-2 rocket data, it was obtained that $T_i \sim 10^4$ K.

In the 1970s, from the Prognoz data it was obtained that two zones exist in the plasmasphere: inner (at $L < 3$), cold, with the ion temperature lower than 8×10^3 K, and warm outer zone (first called hot zone), where the temperature rather rapidly changes with increasing L and can reach 10^5 K. The electron temperature also rises with increasing L [Decreau et al., 1982]. However, a warm zone can also be absent under prolonged geomagnetically quiet conditions, and temperature remains lower than 10^4 in the entire plasmasphere. The GEOS-1, ISEE-1, and DE-1 data confirm the existence of two thermal zones in the plasmasphere [Gringauz and Bassolo, 1990].

Ion temperature in the plasmasphere was studied most thoroughly based on the data of the RIMS/DE-1 ion mass spectrometer with a retarding potential [Comfort, 1986, 1996]. The DE-1 satellite was launched into the circumpolar orbit and twice crossed the same flux tube in each orbit: at low and high altitudes. The dawn and dusk MLT sectors were studied in detail, and the following results were obtained: (1) the plasmaspheric ion temperature is higher than the values typical of the ionosphere in the region of the main density maximum (of the *F* region); (2) the plasmaspheric ion temperature mainly rises with increasing L, and an increase in magnetic activity results in a rise in the temperature in the outer plasmasphere ($L > 3$); (3) the ion temperature on average rises along the magnetic field at a rate of ~0.05–1.0 K km^{-1}, but in the dawn sector the field-aligned temperature gradient is observed only in the outer region ($L > 3$); (4) ion heating sources exist near the equatorial plane; (5) the ion temperature in the inner plasmasphere is subjected to daily variations (see also Fig. 8); (6) the ion temperature in the outer plasmasphere is less stable, independent of the local time, and depends rather on the distance from the plasmapause; (7) the temperatures of H^+, He^+, and O^+ are very close (Fig. 9).

A comparison with the data on density distribution in the plasmasphere apparently indicates that the regimes in the inner ($L < 2.8$–3.0) and outer regions of the plasmasphere are generally different. The inner region is more stable and less subjected to the effect of geomagnetic storms. The parameters of the outer plasmasphere are more variable and less dependent on the processes of ionospheric–plasmaspheric exchange but substantially depend on the interaction between thermal and ring-current plasmas.

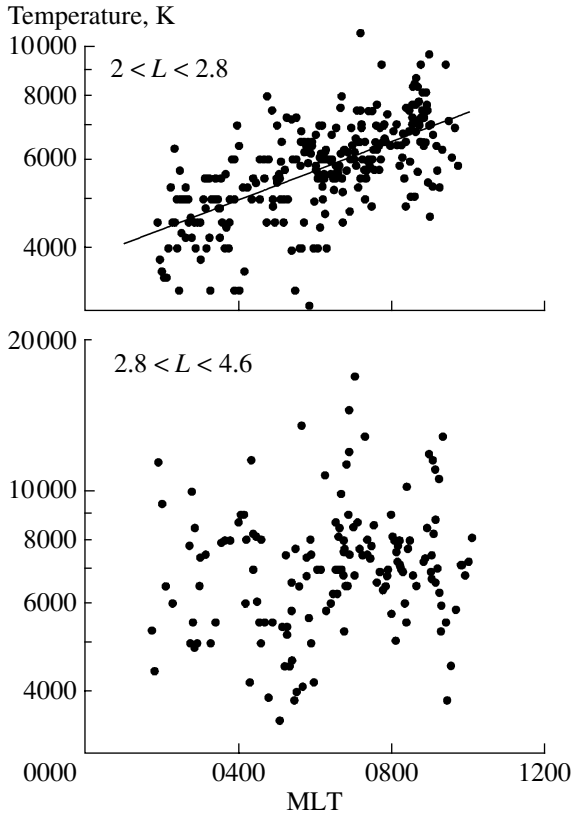

Fig. 8. Proton temperature dependence on magnetic local time (MLT) on the dawn side of the inner and outer plasmaspheric regions according to the INTERBALL-1 data [Kotova et al., 2002].

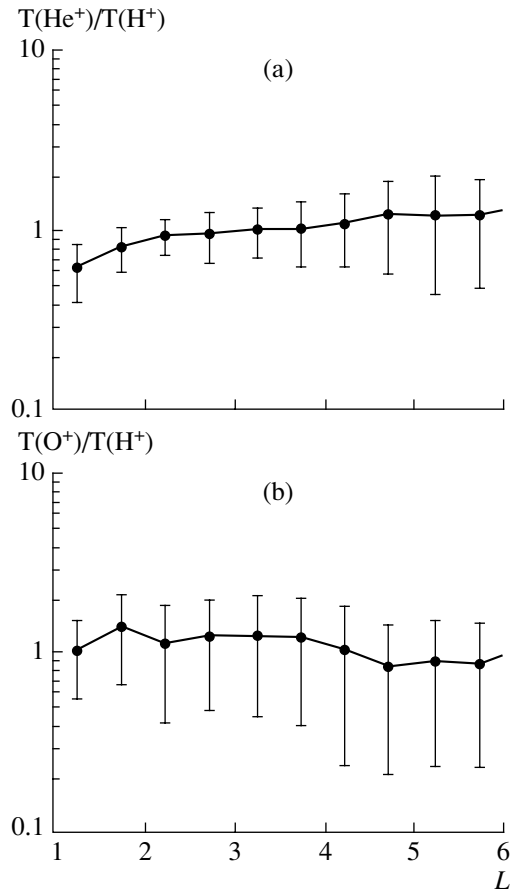

Fig. 9. Average ratios of temperatures of ions (a) He^+ and H^+ and (b) O^+ and H^+ according to the DE-1/RIMS data [Comfort, 1996].

According to the DE-1 data [Comfort, 1986, 1996], additional admixture of suprathermal plasma was often observed in the outer plasmasphere (Fig. 10). The density of this suprathermal component is much lower than that of the cold component.

The data on the ion temperature, obtained in geosynchronous orbit with a magnetospheric plasma analyzer of the Los Alamos National Laboratory (LANL MPA), indicated that a higher ion temperature is usually observed in the regions of decreased density, and, vice versa, decreased temperatures correspond to the regions with increased densities. In this case warmer rarefied regions are much more variable and structured [Gringauz, 1983; Moldwin et al., 1995].

Certain features of the plasmaspheric thermal structure were revealed from the ISEE-1 data. On the dayside, temperature decreased in the inner plasmasphere ($L < 3$) [Comfort, 1986]. So large negative temperature gradients were never observed in the DE-1 data. According to the ISEE-1 data an ion temperature minimum was sometimes observed at $L \sim 4$.

The dependence of the plasmaspheric ion temperature on magnetic activity has been studied rather poorly. The DE-1 data indicate that the temperature decreased at $L > 2$ in the dusk sector at increased magnetic disturbance; on the other hand, increased magnetic activity apparently leads to an increase in temperature at $L > 3$. In the dawn sector, the effect of magnetic activity on ion temperature has not been revealed at $L < 3$; however, temperature rises with increasing magnetic activity at $L > 3$ as in the dusk sector [Comfort, 1996]. We should note that the statistics of cases with high magnetic disturbance is much poorer than the statistics for quiet conditions. Moreover, the time from the beginning and the disturbance phase are substantial in an analysis of the thermal structure of the plasmasphere. Therefore, we should analyze temperature variations during specific passes through the plasmasphere rather than seek statistical dependences.

The dynamics of the proton temperature in the nightside plasmasphere during moderate magnetic disturbances was considered in [Kotova et al., 2006] based on the INTERBALL-2 data. It turned out that, on the nightside of the inner plasmasphere, the temperature decreases during the development of the storm main phase, becomes even higher than the prestorm values under quiet conditions during the recovery phase, and subsequently returns to approximately initial values

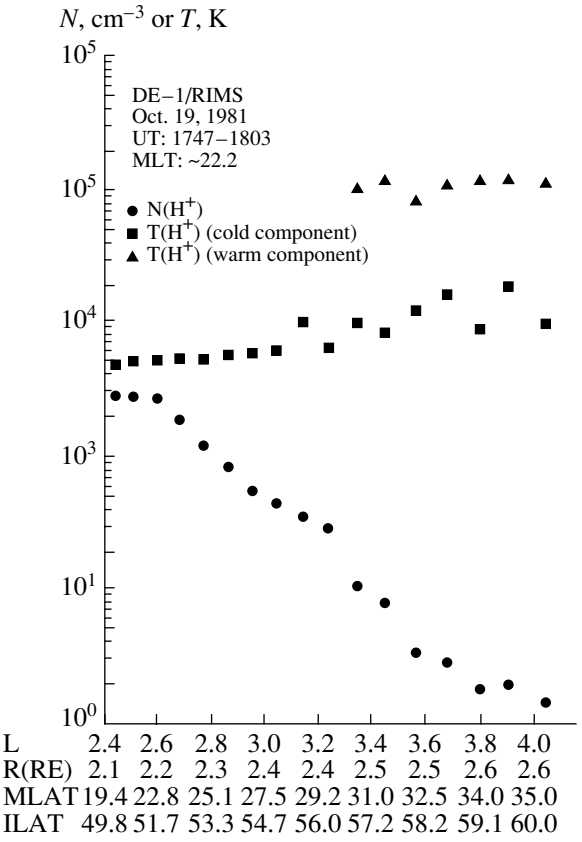

Fig. 10. Distribution of temperature and density of H^+ ions with the additional high-temperature component according to the DE-1/RIMS data [Comfort, 1996].

(Fig. 11). Temperature drop during the storm main phase is possibly related to a change in the plasma flow direction and plasmasphere filling with cold (~1000 K) ionospheric plasma. The following temperature rise is probably related to heating of the plasmaspheric plasma near the equatorial plane, possibly, due to the interaction of this plasma with the ring current plasma.

In spite of the fact that it is very important to know electron temperature in order to study the processes of ionospheric–plasmaspheric exchange, experimental data on electron temperature in the plasmasphere are even poorer than the data on ion temperature. Detailed data on electron temperature at high altitudes (to ~10000 km, $L \sim 2.5$) were obtained only on the EXOS D (AKEBONO) satellite, but these data are reliable only if the electron density is higher than 1000 cm^{-3} [Balan et al., 1996].

The AKEBONO data indicate that (as the temperature of ions) the electron temperature shows diurnal variations in the inner plasmasphere: the daytime temperatures are higher than the nightside ones by a factor of 1.5–2.5 depending on latitude and altitude. The daytime temperature rapidly increases with altitude increasing to ~2500 km and rises much slower above this altitude. On the contrary, the nightside temperature the lower plasmasphere (to ~2500 km) is in the state of approximate thermal equilibrium; above this altitude, the temperature slowly rises at approximately the same velocity as on the dayside. To explain the observed temperature values, Balan et al. [1996] had to introduce the additional altitude-dependent increasing coefficient of

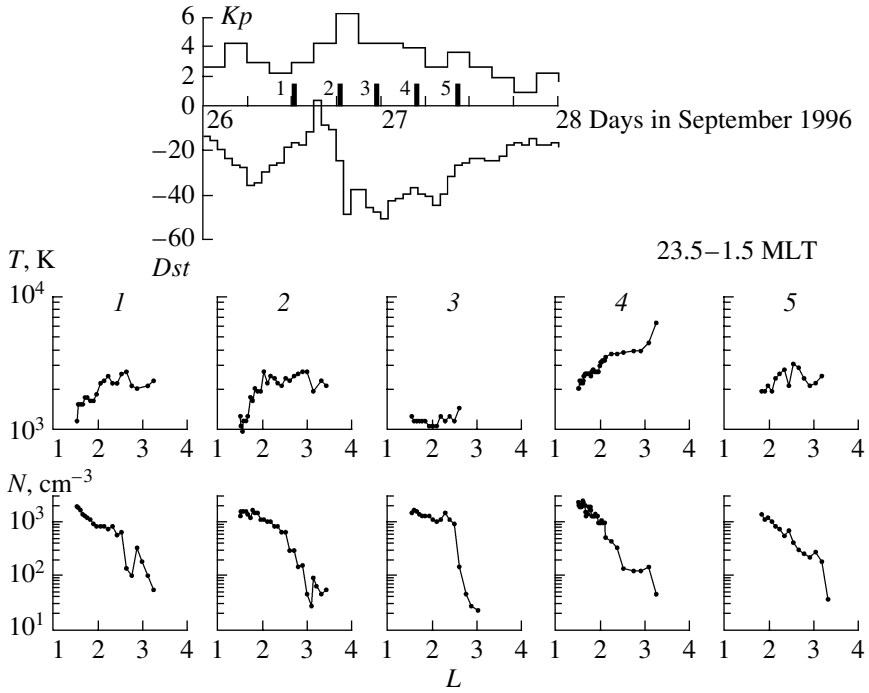

Fig. 11. Ion temperature and density distributions in the Earth's plasmasphere registered during the successive (at an interval of ~6 h) passes of INTERBALL-2 through the nightside plasmasphere during the development of a small magnetic storm.

heat transfer from photoelectrons to background plasma electrons.

An analysis of the AKEBONO data also indicates that geomagnetic activity does not affect electron temperature values at $L < 2.2$. However, the electron temperature above 2000 km altitude increases with increasing $F_{10.7}$ solar flux. It is indicated that the nighttime electron temperature is possibly asymmetric: the temperature is higher in the Southern Hemisphere than in the Northern one; the correlation is apparently inverse for daytime temperatures [Denton et al., 1999].

All experimental data indicate that the ion and electron temperatures are substantially higher in the outer plasmasphere ($L > 3$) than in the ionosphere. There are several causes of an expected increase in the temperature with increasing altitude along field lines, i.e., near the equatorial plane: (1) only sufficiently hot particles can overcome a gravitational barrier, (2) light ions are accelerated by the electric field of ambipolar diffusion generated by oxygen ions and electrons, (3) as a result of a decrease in the effective section of Coulomb collisions with increasing relative particle velocity, high-energy particles can easier leave the ionosphere and escape into the plasmasphere [Lemaire and Gringauz, 1998]. The latter fact becomes more substantial if we assume that the particle velocity distribution is power-low (κ-distribution) in the high-velocity part rather than Maxwellian [Pierrard and Lemaire, 1996].

Nevertheless, the detailed calculations, performed using different models in order to compare with experimental data, indicate that an additional source of ion and electron heating should exist near the equatorial plane, especially near the plasmapause, during magnetically disturbed periods [Comfort, 1996]. Both Coulomb collisions with higher-energy ring current ions [Kozyra, 1987] and different ion–wave interactions [Khazanov et al., 1996] are considered as such a source.

8. CONCLUSIONS

In this review we did not try to consider all problems of physics of the plasmasphere. We did not consider here the problems of a charge and mass composition of the plasmaspheric plasma, measurements and estimates of flows from the ionosphere into the plasmasphere and backward, wave processes in the plasmasphere, etc. An extensive bibliography should make it possible to find references to the studies of interest. The review was mainly aimed at indicating that the plasmasphere is a sufficiently large and substantial part of the Earth's magnetosphere, where the processes proceeding in the Sun and solar wind are related to those in the Earth's ionosphere and atmosphere. In this case several fundamental problems of physics of the plasmasphere remain unclear. A common opinion on the processes responsible for the plasmapause formation, plasmapause filling and erosion, and thermal balance is absent; it is unclear what parts of plasma are discharged into the ionosphere and escape into the outer magnetosphere during magnetic storms. The number of questions that have been accumulated during several decades of studies of the Earth's plasmasphere is so large (as compared to the number of answers) that the plasmasphere waits for its new discovery according to D. Carpenter, one of the pioneers and permanent researchers of this magnetospheric region [Carpenter, 1995].

ACKNOWLEDGMENTS

This work was supported by the Russian Foundation for Basic Research (project no. 04-02-16666a) and the P16/2 RAN and OFN-16 programs.

REFERENCES

1. J. J. Angerami and J. O. Thomas, "Studies of Planetary Atmospheres. 1: The Distributions of Electrons and Ions in the Earth's Exosphere," J. Geophys. Res. **69**, 4537–4560 (1964).
2. G. J. Bailey, N. Balan, and Y. Z. Su, "The Sheffield University Plasmasphere Ionosphere Model: A Review," J. Atmos. Sol.–Terr. Phys. **59**, 1541–1552 (1997).
3. N. Balan, K. I. Oyama, G. J. Bailey, and T. Abe, "Plasmasphere Electron Temperature Studies Using Satellite Observations and Theoretical Model," J. Geophys. Res. **101**, 15 323–15 330 (1996).
4. S. G. Bauer, *Physics of Planetary Ionospheres* (Springer, 1973; Mir, Moscow, 1976).
5. V. V. Bezrukikh, M. I. Verigin, G. A. Kotova, et al., "Dynamics of the Plasmasphere and Plasmapause under the Action of Geomagnetic Storms," J. Atmos. Sol.–Terr. Phys. **63**, 1179–1184 (2001).
6. L. P. Block, "On the Distribution of Electric Fields in the Magnetosphere," J. Geophys. Res. **71**, 855–864 (1966).
7. N. M. Brice, "Bulk Motion of the Magnetosphere," J. Geophys. Res. **72**, 5193–5211 (1967).
8. J. L. Burch, J. Goldstein, and B. R. Sandel, "Cause of Plasmasphere Corotation Lag," Geophys. Res. Lett. **31**, L05802 (2004).
9. D. L. Carpenter and C. G. Park, "On What Ionospheric Workers Should Know about the Plasmapause–Plasmasphere," Rev. Geophys. Space Phys. **11**, 133–154 (1973).
10. D. L. Carpenter and J. Lemaire, "Erosion and Recovery of the Plasmasphere in the Plasmapause Region," Space Sci. Rev. **80**, 153–179 (1997).
11. D. L. Carpenter and R. R. Anderson, "An ISEE Whistler Model of Equatorial Electron Density in the Magnetosphere," J. Geophys. Res. **97**, 1097–1108 (1992).
12. D. L. Carpenter, "Remote Sensing the Earth's Plasmasphere," Radio Sci. Bul. **308**, 13–29 (2004).
13. D. L. Carpenter, "The Earth's Plasmasphere Awaits Rediscovery," EOS **76**, 89 (1995).
14. D. L. Carpenter, "Whistler Evidence of a 'Knee' in the Magnetospheric Ionization Density Profile," J. Geophys. Res. **68**, 1675–1682 (1963).
15. D. L. Carpenter, "Whistler Studies of the Plasmapause in the Magnetosphere. I. Temporal Variations in the Posi-

tion of the Knee and Some Evidence on Plasma Motions near the Knee," J. Geophys. Res. **71**, 693–709 (1966).

16. D. L. Carpenter, "Whistler Measurements of the Equatorial Profile of Magnetospheric Electron Density," in *Progress in Radio Science 1960–1963, Vol. III: The Ionosphere*, Ed. by G. M. Brown, (Elsevier, Amsterdam, 1965), pp. 76–91.
17. D. L. Carpenter, B. L. Giles, C. R. Chappell, et al., "Plasmaspheric Dynamics in the Duskside Bulge Region: A New Look at an Old Topic," J. Geophys. Res. **98**, 19243–19271 (1993).
18. C. R. Chappell, S. A. Fields, C. R. Baugher, et al., "The Retarding Ion Mass Spectrometer on Dynamics Explorer-A," Space Sci. Instrum. **5**, 477–491 (1981).
19. A. J. Chen and J. M. Grebowsky, "Dynamical Interpretation of Observed Plasmasphere Deformations," Planet. Space Sci. **26**, 661–672 (1978).
20. A. J. Chen and R. A. Wolf, "Effects on the Plasmasphere of Time-Varying Convection Electric Field," Planet. Space Sci. **20**, 483–459 (1972).
21. R. H. Comfort, "Plasmasphere Thermal Structure as Measured by ISEE-1 and DE-1," Adv. Space Res. **6**, 31–40 (1986).
22. R. H. Comfort, "Thermal Structure of the Plasmasphere," Adv. Space Res. **17**, (10)175–(10)184 (1996).
23. P. M. E. Decreau, C. Beghin, and M. Parrot, "Global Characteristics of the Cold Plasma in the Equatorial Plasmapause Region as Deduced from the GEOS 1 Mutual Impedance Probe," J. Geophys. Res. **87**, 695–712 (1982).
24. M. H. Denton, G. J. Bailey, Y. Z. Su, et al., "High Altitude Observations of Electron Temperature and Possible North–South Asymmetry," J. Atmos. Sol.–Terr. Phys. **61**, 775–788 (1999).
25. D. L. Gallagher, M. L. Adrian, and M. W. Liemohn, "Origin and Evolution of Deep Plasmaspheric Notches," J. Geophys. Res. **110**, A09201 (2005).
26. D. L. Gallagher, P. D. Craven, and R. H. Comfort, "Global Core Plasma Model," J. Geophys. Res. **105**, 18 819–18 883 (2000).
27. J. Goldstein, B. R. Sandel, W. T. Forrester, and P. H. Reiff, "IMF-Driven Plasmasphere Erosion of 10 July 2000," Geophys. Res. Lett. **30**, 1146 (2003).
28. J. Goldstein, B. R. Sandel, and M. F. Thomsen, et al., "Simultaneous Remote Sensing and in situ Observations of Plasmaspheric Drainage Plumes," J. Geophys. Res. **109**, A03202 (2004).
29. J. M. Grebowsky, "Model Study of Plasmapause Motion," J. Geophys. Res. **75**, 4329–4333 (1970).
30. J. L. Green and B. W. Reinisch, "An Overview of Results from the RPI on IMAGE," Space Sci. Rev. **109**, 183–210 (2003).
31. J. L. Green, B. R. Sandel, S. F. Fung, et al., "On the Origin of Kilometric Continuum," J. Geophys. Res. **107**, 1029 (2002).
32. K. I. Gringauz and V. S. Bassolo, "Structure and Properties of the Earth's Plasmasphere: Experimental Data and Problems of Their Interpretation (a Review)," Geomagn. Aeron. **30** (1), 1–17 (1990).
33. K. I. Gringauz and V. V. Bezrukikh, "Asymmetry of the Earth's Plasmasphere in the Direction Noon–Midnight from PROGNOZ-1 and PROGNOZ-2 Data," J. Atmos. Terr. Phys. **38**, 1071–1076 (1976).
34. K. I. Gringauz and V. V. Bezrukikh, "The Earth's Plasmasphere: A Review," Geomagn. Aeron. **17**, 784–803 (1977).
35. K. I. Gringauz, "Plasmasphere and Its Interaction with the Ring Current," Space Sci. Rev. **34**, 245–257 (1983).
36. K. I. Gringauz, "Rocket Measurements of Electron Density in the Ionosphere Using UHF Dispersion Interferometer," Dokl. Akad. Nauk SSSR **120**, 1934–1938 (1958).
37. K. I. Gringauz, V. V. Bezrukikh, V. D. Ozerov, and R. E. Rybchinskii, "Studying the Interplanetary Ionized Gas, Energetic Electrons, and Solar Corpuscular Radiation Using Three-Electrode Traps of Charged Particles on the Second Soviet Space Rocket," Dokl. Akad. Nauk SSSR **131**, 1302–1304 (1960).
38. K. I. Gringauz, V. V. Bezrukikh, and V. D. Ozerov, "Positive Ion Density Measurements in the Ionosphere Using the Method of Ion Traps on the Third Soviet Satellite," Iskusstv. Sputniki Zemli **6**, 63–100 (1961).
39. S. M. Guitter, C. E. Rasmussen, T. I. Gombosi, et al., "What Is the Source of Observed Annual Variations in Plasmaspheric Density?," J. Geophys. Res. **100**, 8013–8020 (1995).
40. D. A. Gurnett, R. R. Anderson, F. L. Scarf, et al., "Initial Results Form ISEE-1 and -2 Plasma Wave Investigation," Space Sci. Rev. **23**, 103–122 (1979).
41. B. Higel and L. Wu, "Electron Density and Plasmapause Characteristics at 6.6 R_E: A Statistical Study of the GEOS-2 Relaxation Sounder Data," J. Geophys. Res. **89**, 1583–1601 (1984).
42. *Introduction to Space Physics*, Ed. by M. G. Kivelson and C. T. Russell (Univ. Press, Cambridge, 1995).
43. E. T. Karlson, "Plasma Flow in the Magnetosphere. 1. A Two Dimensional Model of Stationary Flow," Cosmic Electrodyn. **1**, 474–495 (1971).
44. G. V. Khazanov, J. U. Kozyra, and O. A. Gorbachev, "Magnetospheric Convection and the Effects of Wave–Particle Interaction on the Plasma Temperature Anisotropy in the Equatorial Plasmasphere," Adv. Space Res. **17**.
45. G. V. Khazanov, M. V. Liemohn, J. U. Kozyra, and T. E. Moore, "Inner Magnetospheric Superthermal Electron Transport: Photoelectron and Plasma Sheet Electron Sources," J. Geophys. Res. **103**, 23 485–23 501 (1998).
46. G. Kotova, V. Bezrukikh, M. Verigin, and J. Šmilauer, "In situ Observations of Low-Density Regions Inside the Plasmasphere," Earth Planet. Space **56**, 989–996 (2004).
47. G. Kotova, V. Bezrukikh, M. Verigin, and J. Šmilauer, "Ion Temperature Dynamics in the Plasmasphere from INTERBALL Measurements during Minimum and Maximum Phases of Solar Cycle," in *Proceedings of the International Symposium on Recent Observations and Simulations of the Sun–Earth System, Varna, 2006*, p. 62.
48. G. A. Kotova, V. V. Bezrukikh, M. I. Verigin, et al., "INTERBALL 1 / Alpha 3 Cold Plasma Measurements in the Evening Plasmasphere: Quiet and Disturbed Magnetic Conditions," Adv. Space Res. **30**, 2002 (2002).
49. G. A. Kotova, V. V. Bezrukikh, M. I. Verigin, and L. A. Lezhen, "Temperature and Density Variations in

the Dusk and Dawn Plasmasphere as Observed by INTERBALL–TAIL in 1999–2000," Adv. Space Res. **30**, 1831–1834 (2002).

50. J. U. Kozyra, E. G. Shelley, R. H. Comfort, et al., "The Role of Ring Current O+ in the Formation of Stable Auroral Red Arcs," J. Geophys. Res. **92**, 7487–7502 (1987).
51. I. A. Krinberg and A. V. Tashchilin, *The Ionosphere and Plasmasphere* (Nauka, Moscow, 1984) [in Russian].
52. J. F. Lemaire and K. I. Gringauz, with contribution from D. L. Carpenter and V. Bassolo *The Earth's Plasmasphere* (Cambridge Univ. Press, Cambridge, 1998).
53. J. F. Lemaire, "Hydrostatic Equilibrium and Convective Stability in the Plasmasphere," J. Atmos. Sol.–Terr. Phys. **61**, 867–878 (1999).
54. J. F. Lemaire, "The Formation of Light-Ion Trough and Peeling of the Plasmasphere," J. Atmos. Sol.–Terr. Phys. **63**, 1285–1291 (2001).
55. J. F. Lemaire, "The Formation of Plasmaspheric Tails," Phys. Chem. Earth (C) **25**, 9–17 (2000).
56. M. W. Liemohn, A. J. Ridley, D. L. Gallagher, et al., "Dependence of Plasmaspheric Morphology on the Electric Field Description during the Recovery Phase of the 17 April 2002 Magnetic Storm," J. Geophys. Res. **109**, A03209 (2004).
57. C. E. McIlwain, "A *Kp* Dependent Equatorial Electric Field Model," Adv. Space Res. **6** (3), 187–197 (1986).
58. M. B. Moldwin, L. Downward, H. K. Rassoul, et al., "A New Model of the Location of the Plasmapause: CRRES Results," J. Geophys. Res. **107**, 1339 (2002).
59. M. B. Moldwin, M. F. Thomse, S. J. Bame, et al., "The Fine Scale Structure of the Outer Plasmasphere," J. Geophys. Res. **100**, 8021–8029 (1995). Correction, J. Geophys. Res. **100**, 9649 (1995).
60. A. Nishida, "Formation of Plasmapause, or Magnetospheric Plasma Knee, by the Combined Action of Magnetospheric Convection and Plasma Escape Form the Tail," J. Geophys. Res. **71**, 5669–5679 (1966).
61. C. G. Park, "Some Features of Plasma Distribution in the Plasmasphere Deduced from Antarctic Whistlers," J. Geophys. Res. **79**, 169–173 (1974).
62. C. G. Park, D. L. Carpenter, and D. B. Wiggin, "Electron Density in the Plasmasphere: Whistler Data on the Solar Cycle, Annual, and Diurnal Variations," J. Geophys. Res. **83**, 3137–3144 (1978).
63. V. Pierrard and J. Lemaire, "Development of Shoulders and Plumes in the Frame of the Interchange Instability Mechanism for Plasmapause Formation," Geophys. Res. Lett. **31**, L05809 (2004).
64. V. Pierrard and J. Lemaire, "Exospheric Model of the Plasmasphere," J. Atmos. Sol.–Terr. Phys. **63**, 1261–1265 (2001).
65. V. Pierrard and J. Lemaire, "Lorentzian Ion Exosphere Model," J. Geophys. Res. **101**, 7923–7934 (1996). Correction, J. Geophys. Res. **103**, 4117 (1998).
66. C. E. Rasmussen, S. M. Guitter, and S. G. Thomas, "A Two-Dimensional Model of the Plasmasphere: Refilling Time Constants," Planet. Space Sci. **41**, 35–43 (1993).
67. M. A. Reynolds, D. J. Melendez-Alvira, and G. Ganguli, "Equatorial Coupling between the Plasmasphere and the Topside Ionosphere," J. Atmos. Sol.–Terr. Phys. **63**, 1267–1273 (2001).
68. P. G. Richards and D. G. Torr, "Hydrodynamic Model of the Plasmasphere," Geophys. Monogr. Am. Geophys. Union, No. 44, 67–77 (1988).
69. P. G. Richards, T. Chang, and R. H. Comfort, "On the Causes of the Annual Variation in the Plasmaspheric Electron Density," J. Atmos. Sol.–Terr. Phys. **62**, 935–946 (2000).
70. B. R. Sandel, J. Goldstein, D. L. Gallagher, and M. Spasojevic, "Extreme Ultraviolet Imager Observations of the Structure and Dynamics of the Plasmasphere," Space Sci. Rev. **109**, 25–46 (2003).
71. R. W. Schunk and J. J. Sojka, "Ionospheric Models," in *Modern Ionospheric Science*, Ed. by H. Kohl, R. Ruster, and K. Schlegel (EGS, Katlenburg-Lindau, 1996), pp. 181–215.
72. X. Song, R. Gendrin, and G. Caudal, "Refilling Process in the Plasmasphere and Its Relation to Magnetic Activity," J. Atmos. Terr. Phys. **50**, 185–195 (1988).
73. R. W. Spiro, M. Harel, R. A. Wolf, and P. H. Reiff, "Quantitative Simulation of Magnetospheric Substorm. 3. Plasmaspheric Electric Fields and Evolution of the Plasmapause," J. Geophys. Res. **86**, 2261–2272 (1981).
74. L. R. Storey, "An Investigation of Whistling Atmospherics," Phil. Trans. Roy Soc. (London), Ser. A: **246**, 113–141 (1953).
75. Gy. Tarcsay, P. Szemeredy, and L. Hegymegi, "Average Electron Density Profiles in the Plasmasphere between $L = 1.4$ and 3.2 Deduced from Whistlers," J. Atmos. Terr. Phys. **50**, 607–611 (1988).
76. J.-N. Tu, J. L. Horwitz, P. Song, et al., "Simulating Plasmaspheric Field-Aligned Density Profiles Measured with IMAGE/RPI: Effects of Plasmasphere Refilling and Ion Heating," J. Geophys. Res. **108**, 1017 (2003).
77. P. A. Webb and E. A. Essex, "A Dynamic Global Model of the Plasmasphere," J. Atmos. Sol.–Terr. Phys. **66**, 1057–1073 (2004).
78. J. Wygant, D. Rowland, H. J. Singer, et al., "Experimental Evidence on the Role of the Large Spatial Scale Electric Field in Creating the Ring Current," J. Geophys. Res. **103**, 29 527–29 544 (1998).